The Logarithmic Triviality of Compact QED Coupled to a Four-Fermi Interaction

John B. Kogut[a] **and Costas G. Strouthos**[b]

[a] *Physics Department, University of Illinois at Urbana-Champaign,*
Urbana, IL 61801-30.

[b] *Department of Physics, University of Cyprus,*
CY-1678 Nicosia, Cyprus.

Abstract

This is the completion of an exploratory study of Compact lattice Quantum Electrodynamics with a weak four-fermi interaction and four species of massless fermions. In this formulation of Quantum Electrodynamics massless fermions can be simulated directly and Finite Size Scaling analyses can be performed at the theory's chiral symmetry breaking critical point. High statistics simulations on lattices ranging from 8^4 to 24^4 yield the equation of state, critical indices, scaling functions and cumulants. The measurements are well fit with the orthodox hypothesis that the theory is logarithmically trivial and its continuum limit suffers from Landau's zero charge problem.

PACS: 12.38.Mh, 12.38.Gc, 11.15.Ha

1

1 Introduction

This is the final paper in a series of simulation studies searching for a nontrivial ultra-violet fixed point in abelian gauge theories. Previous studies have provided simulation evidence that scalar QED [1] and noncompact lattice QED with four species of massless fermions [2] are logarithmically trivial.

This work employs the χQED formulation of the model in which a weak four-fermi interaction is added to the standard action. This affords us two advantages over standard methods: 1. we can simulate massless fermions directly on the lattice and see how massless fermion charge screening affects the dynamics, and 2. the four-fermi interaction separates the chiral transition of the model from its confinement/deconfinement transition which is a first order transition and is controlled by monopole condensation.

The χQED action contains two couplings, $\beta = 1/e^2$ where e is the usual electrodynamic charge, and the four-fermi coupling, $G = 1/\lambda$. The model's phase diagram contains two separate lines of transitions, one describing monopole condensation which is first order and a line of second order chiral transitions. We will show that the line of second order chiral transitions describes a logarithmically trivial continuum limit, presumably identical to the continuum limit of the noncompact χQED lattice model studied earlier [2].

This will be accomplished by exploiting the fact that Finite Size Scaling (FSS) applies simply to χQED because it is formulated without a bare fermion mass. In the conventional lattice action the bare fermion mass explicitly breaks chiral symmetry and introduces scale breaking. A nonzero fermion mass is needed so that the standard algorithm converges. By contrast, χQED allows us to study the physics of the critical point by doing simulations in its immediate vicinity and extracting information from FSS arguments without ever needing uncontrolled extrapolations to the chiral limit. One of the purposes of this paper is the illustration of FSS methods for lattice gauge theories with massless fermions. This represents new territory for lattice gauge theory.

Of course, this work is not without its disappointments. We cannot simulate the model in a range of parameters where monopoles are relevant degrees of free-

dom in the theory's continuum limit. For this action, the line of monopole condensation transitions is distinct from that of the chiral transitions and monopole condensation appears to be first order. It has been argued elsewhere [4] that a second order transition where there is both chiral symmetry breaking and monopole condensation would be a natural scenario for a nontrivial form of continuum QED because screening effects coming from fermions could balance anti-screening effects coming from monopoles. A future formulation of lattice monopoles and fermions will have to be developed to see if this possibility could work out.

Since this paper is a continuation in a series we refer the reader to reference [3] for additional background and formulas. Here our emphasis is on the new simulations, FSS methods and results.

The paper begins by laying out the lattice theory's two dimensional phase diagram and presenting some simulations which pin down its qualitative features. Then some highly accurate 16^4 and 24^4 simulations in the broken symmetry phase are presented and analyzed. This is the approach used in past studies which showed that the noncompact model is logarithmically trivial [2]. The compact model should also be logarithmically trivial because the chiral transition occurs in a region of the model's phase diagram where monopoles are not critical. Under these conditions the differences between the compact and noncompact models should become irrelevant and the models should have the same continuum limit [5]. This conventional idea was not well supported by our first simulation study [3] of the model which motivated us to do a more thorough job which we report here. The conclusions presented here are based on over ten times the statistics of earlier work. High statistics allowed the simulation program to reach thermodynamic equilibrium and produce more accurate ensembles of configurations which reduced the error bars substantially. The 16^4 and 24^4 data in the broken symmetry phase can be fit with both power laws whose critical indices deviate from mean field theory, as reported in [3], *or* log-improved mean field theory. The log-improved mean field theory fits are somewhat better than the power law fits, but a conclusive result eludes us if we just use this subset of our simulations. However, the combination of the broken phase results together with new simulations,

3

analyzed with FSS methods on lattices ranging from 8^4 to 16^4, in the immediate vicinity of the model's critical point lead to stronger results: they favor the logarithmically trivial fermionic field theory scenario. This is the new conclusion which will be presented below.

This paper is organized as follows: In the next section we briefly review the formulation of the lattice action and define the parameters we use in our fits and simulations. In the third section we sketch the phase diagram and present a few simulations which led to it. Then we examine several points in the phase diagram along the line of chiral transitions and show that the data for the chiral order parameter in the broken symmetry phase is compatible with log-improved mean field theory. Next we review the relevant features of FSS and present several sections of analysis of high statistics data sets using lattices ranging from 8^4 through 16^4. This is the most decisive analysis in this study. Its success depended crucially on the use of the χQED action and statistically large data sets which are several orders of magnitude larger than those used in typical lattice simulations of QCD, for example. FSS simulations at and near the critical coupling were essential to establishing the logarithmic triviality of this model.

2 Formulation

The lattice Action of compact χQED, where the gauge symmetry is interpreted as a compact local $U(1)$ symmetry, following Wilson's original proposal [6], reads

$$S = \sum_{x,y} \bar{\psi}(x)(M_{xy}+D_{xy})\psi(y)+\frac{1}{2G}\sum_{\tilde{x}}\sigma^2(\tilde{x})+\frac{1}{2e^2}\sum_{x,\mu,\nu}(1-\cos(F_{\mu\nu}(x))), (1)$$

where

$$F_{\mu\nu}(x) = \theta_\mu(x) + \theta_\nu(x + \hat{\mu}) + \theta_{-\mu}(x + \hat{\mu} + \hat{\nu}) + \theta_{-\nu}(x + \hat{\nu}), \quad (2)$$

$$M_{xy} = (m + \frac{1}{16}\sum_{\langle x,\tilde{x}\rangle}\sigma(\tilde{x}))\delta_{xy}, \quad (3)$$

$$D_{xy} = \frac{1}{2}\sum_{\mu}\eta_\mu(x)(e^{i\theta_\mu(x)}\delta_{x+\hat{\mu},y} - e^{-i\theta_\mu(y)}\delta_{x-\hat{\mu},y}). \quad (4)$$

The auxiliary scalar field σ is defined on the sites of the dual lattice $\tilde{x}$ [7], and the symbol $\langle x, \tilde{x} \rangle$ denotes the set of the 16 lattice sites surrounding the direct site x. The factors $e^{\pm i\theta_\mu}$ are the gauge connections and $\eta_\mu(x)$ are the staggered phases, the lattice analogs of the Dirac matrices. ψ is a staggered fermion field and m is the bare fermion mass, which will be set to zero. Note that the lattice expression for $F_{\mu\nu}$ is the circulation of the lattice field θ_μ around a closed plaquette, the gauge field couples to the fermion field through compact phase factors to guarantee local gauge invariance and $\cos F_{\mu\nu}$ enters the action to make it compact.

It will often prove convenient to parametrize results with the inverse of the four-fermi coupling, $\lambda \equiv 1/G$, and the inverse of the square of the gauge coupling, $\beta \equiv 1/e^2$.

The global Z_2 chiral symmetry of the Action reads:

$$\psi(x) \quad \rightarrow \quad (-1)^{x1+x2+x3+x4}\psi(x) \tag{5}$$
$$\bar{\psi}(x) \quad \rightarrow \quad -\bar{\psi}(x)(-1)^{x1+x2+x3+x4} \tag{6}$$
$$\sigma \quad \rightarrow \quad -\sigma. \tag{7}$$

where $(-1)^{x1+x2+x3+x4}$ is the lattice representation of γ_5.

Interesting limiting cases of the above Action are: (i) the Z_2 Nambu$-$Jona-Lasinio model with no gauge fields, set e^2 to zero here, which has a logarithmically trivial chiral phase transition at nonzero G; (ii) the compact QED model with no four-fermi interactions, whose first order chiral phase transition is coincident with its first order monopole condensation transition near $\beta \equiv 1/e^2 \approx 0.89(1)$ for four flavors [9]; and (iii) the $G \rightarrow \infty$ limit in which the fermions obtain a dynamical mass comparable to the reciprocal of the lattice spacing and therefore decouple, leaving quenched compact QED which has a first order transition at $\beta = 1.011124(1)$ [10].

We refer the reader to earlier papers in this series [3] for more motivation and details. We only emphasize new simulations and analyses here.
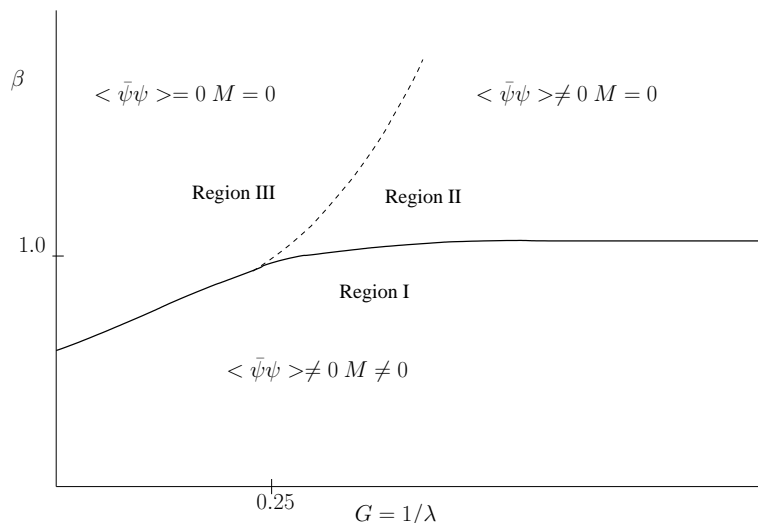
Figure 1: Phase Diagram of Gauged Compact $U(1)$ Nambu Jona-Lasinio Model

3   Overview of the Phase Diagram.

The phase diagram for the model [3] is shown in Fig. 1. The monopole concentration M and the chiral condensate, $\langle \bar{\psi}\psi \rangle$, label the three phases. Region I has chiral symmetry breaking in a condensate of monopoles, Region II has chiral symmetry breaking in a monopole free vacuum, and Region III is chirally symmetric in a monopole free vacuum. Past simulations suggest that the dashed line consists of second order transitions and the thick line consists of first order transitions [3].

It is interesting to confirm that the dashed line of chiral symmetry breaking transitions in the upper reaches of Fig. 1 turns vertical and the four-fermi coupling alone breaks chiral symmetry at strong coupling, in agreement with [8]. This is shown in Fig. 2 where we confirm that the model breaks chiral symmetry for $G = 1.0$ no matter how small the gauge coupling $e^2 = 1/\beta$.

In reference [3] we concentrated on the vertical line $G = 1/1.4$ and showed that the line of first order monopole concentration transitions is clearly separate from the line of chiral symmetry transitions. We felt that it was important to simulate along another vertical line in the phase diagram to verify this result and
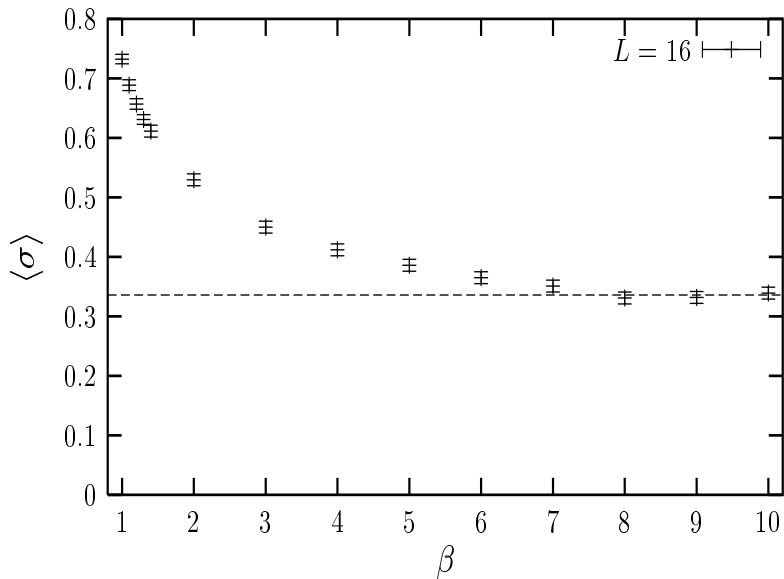
Figure 2: $\langle \sigma \rangle$ vs. gauge coupling $\beta = 1/e^2$ at fixed four-fermi coupling $G = 1.0$.

to see how sensitive the characteristics of the transitions are to the bare couplings. There are several questions we need to address. They include: (i) Does the order of the transition(s) change along the lines in the phase diagram? (ii) Do the critical indices change along the lines? There are related models where this is known to happen, such as in the quenched noncompact gauged Nambu-Jona Lasinio model [11]. It is unknown if such phenomena can occur in unquenched abelian models where fermion screening leads to the zero charge problem in perturbation theory and produces only perturbatively trivial models.

In Fig. 3 we show the monopole concentration as the gauge coupling β passes through the phase boundary at $G = 0.50$ between regions I and II. The monopole concentration appears to have a discontinuous jump just below $\beta = 0.935$.

Measurements of $\langle \sigma \rangle$ in Fig. 4 also show the first order transition near $\beta = 0.935$ and indicate that region II (see Fig. 1) extends from this point to approximately $\beta \approx 0.96$ along the vertical line at $G = 0.50$.

The simulations reported in [3] along the vertical line $G = 1/1.4$ found a continuous chiral transition at $\beta = 1.393(1)$. It is interesting to check the consistency
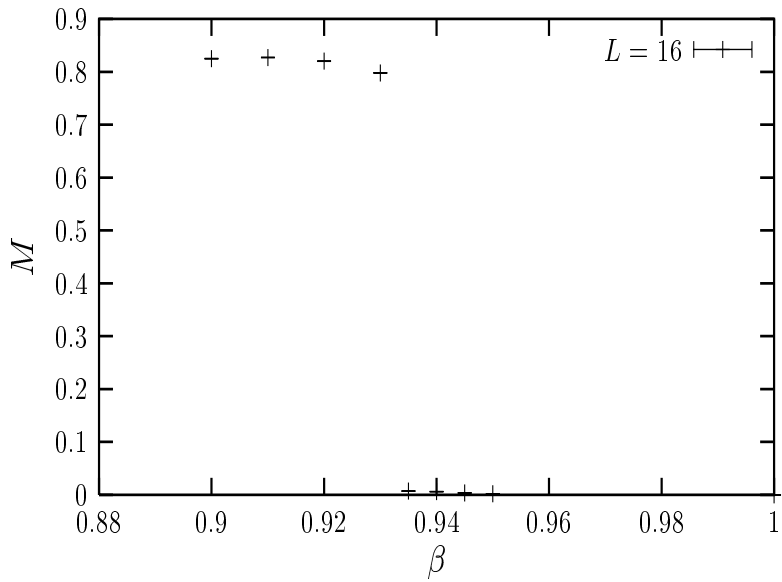
7

Figure 3: Monopole concentration vs. gauge coupling β at fixed four-fermi coupling $G = 0.50$.
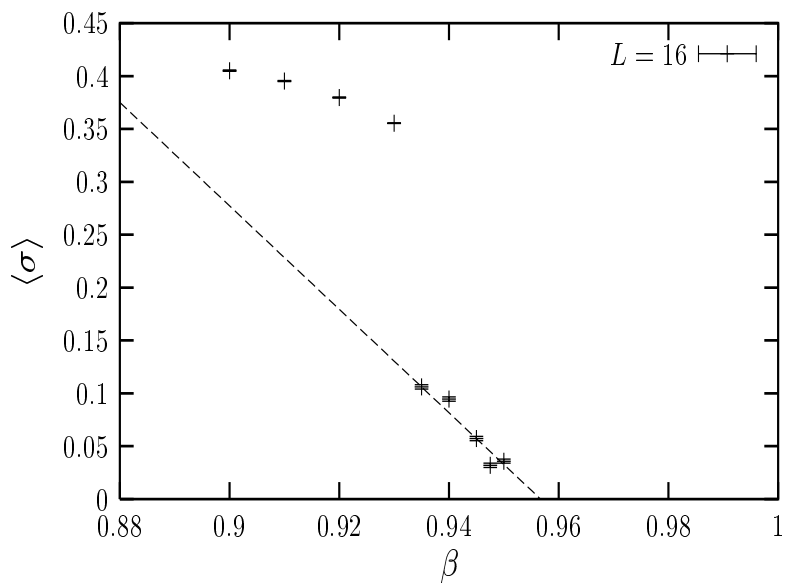

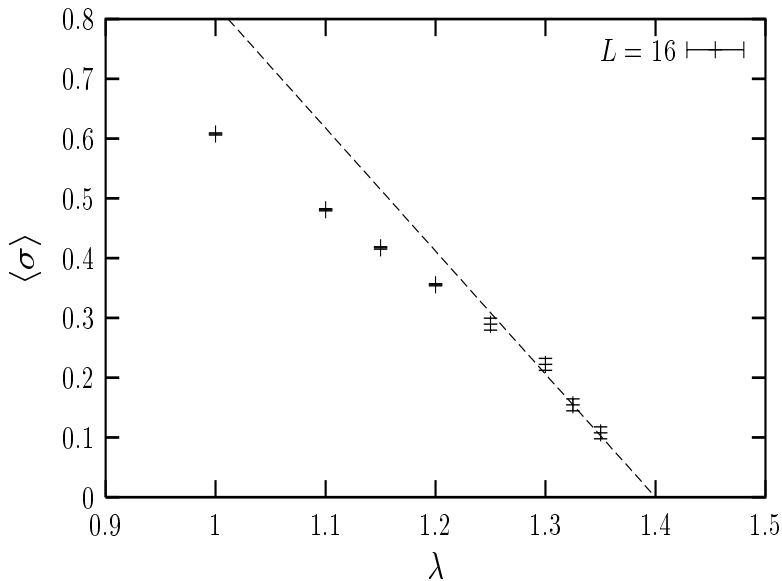Figure 4: $\langle\sigma\rangle$ vs. gauge coupling β at fixed four-fermi coupling $G = 0.50$.

Figure 5: $\langle\sigma\rangle$ vs. four-fermi coupling $\lambda = 1/G$ at fixed gauge coupling $\beta = 1.393$.

of this prediction with simulations approaching the critical point from a different direction in the phase diagram. Therefore, we simulated the model on 16^4 lattices along the horizontal direction, fixing $\beta = 1.393$ and varying the four-fermi coupling. The results are shown in Fig. 5.

We see that Fig. 5, although not competitive in accuracy with the study at fixed four-fermi coupling and variable gauge coupling due to an apparently narrow scaling region, is indeed compatible with the earlier results: the critical point is again predicted to be at $G = 1/1.4$ and $\beta = 1.393$. The dashed curve in Fig. 5 is just meant to guide the eye to the horizontal line.

4   High Statistics 16^4 Simulations along the Vertical Line $\lambda = 1.4$

The real focus of this series of simulations is to determine the quantitative nature of the line of chiral transitions in the phase diagram. We, therefore, developed a very fast, parallel version of the simulation code and made high statistics runs
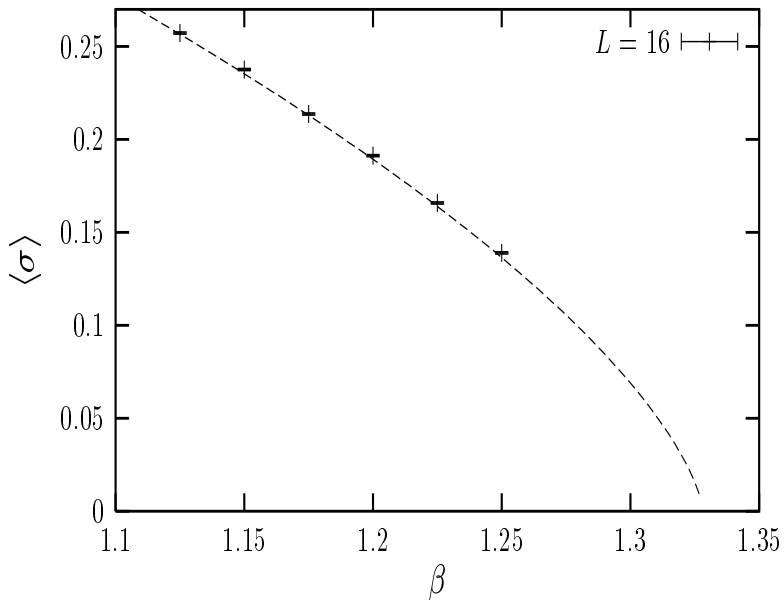
Figure 6: $\langle\sigma\rangle$ vs β at four-fermi coupling $\lambda = 1.4$. The fit has the critical index $\beta_{mag} = 0.65(4)$.

along the vertical line $\lambda = 1.4$, complementing the exploratory runs reported earlier [3]. In fact, between 10×10^6 and 20×10^6 sweeps of the Hybrid Molecular Dynamics algorithm were done at each of fifteen couplings β ranging from $\beta = 1.393$ to $\beta = 1.125$. This is more than an order of magnitude greater statistics than those previously reported and represent between $100,000$ and $200,000$ trajectories of the Hybrid Molecular Dynamics algorithm [12] at each coupling (the Monte Carlo time interval was chosen to be $dt = 0.01$ to keep systematic errors negligible in the molecular dynmics steps). The data on the broken chiral symmetry side of the transition is plotted in Fig. 6 and a power-law fit is included in the figure. (The data on the other side of the transition will be used in a FSS analysis below.) The power-law fit, $\langle\sigma\rangle = A(\beta_c - \beta)^{\beta_{mag}}$, is acceptable, $\chi^2/DOF = 1.7$ with a critical point $\beta_c = 1.33(1)$ and a critical magnetization exponent $\beta_{mag} = 0.65(10)$.

It is interesting that the critical index is larger than the mean field value of $1/2$, but the deviation from mean field theory is less than reported in our earlier, lower statistics, exploratory work [3]. The high statistics of this run are making a

10

difference in the results. We recall from other works using $U(1)$ gauge fields and the simplest Wilson action, that very long relaxation times are noted [10]. Our time correlation analysis suggests that the 20 million sweeps used here suffice and the error bars in the figure conservatively account for the correlations in Monte Carlo time. It is interesting that simulations of the noncompact model [2] did *not* require such enormous statistics to achieve equally accurate results.

Following our analysis of the noncompact model, however, it is interesting to attempt to fit the same data with the hypothesis of logarithmic triviality. As discussed in previous work, including reference [8], the logarithms of triviality effect the scaling laws and equation of state differently for fermionic theories than for bosonic theories. In particular, in references [2, 8], the leading order equation of state had the form $\beta_c - \beta = A\langle\sigma\rangle^2(\ln(1/\langle\sigma\rangle) + B)$. Fits of this form accomodate the data of Fig. 6 very well, in fact, just like in the noncompact model. Fitting routines predict the parameter $B = 0.84(8)$, $A = 7.3(9)$ and $\beta_c = 1.33(1)$ with $\chi^2/DOF = 0.66$. To emphasize the need for the logarithm here, we plot the quantity $(\beta_c - \beta)/\langle\sigma\rangle^2$ against $\ln(1/\langle\sigma\rangle)$ in Fig. 7, and show the fit. This makes the point that the simulation results are compatible with logarithmic triviality. In fact, they appear to rule out bosonic triviality fits which would have the logarithm of triviality in the denominator of the equation, like $\beta_c - \beta = A\langle\sigma\rangle^2/(\ln(1/\langle\sigma\rangle) + B)$, rather than the numerator. Our work, therefore, supports the analytic predictions of A. Koci*ć* [13]. Perhaps, the fact that the χ^2/DOF from the log-improved mean field relation (which is a three-parameter function) is less than half the χ^2/DOF we get from the fit to the standard power-law relation (which is also a three-parameter function) is evidence that the data favor the triviality scenario over the interacting field theory scenario. More compelling and straight-forward evidence for triviality will be presented in the sections on FSS below.

This result is not above criticism, however. As is clear from the figures, we are not able to simulate the model very close to the critical point on this lattice size without meeting uncontrollable finite size effects. For example, simulations closer to β_c display tunneling between the Z_2 vacua through the unbroken phase and make reliable measurements of the order parameter impossible. We will turn
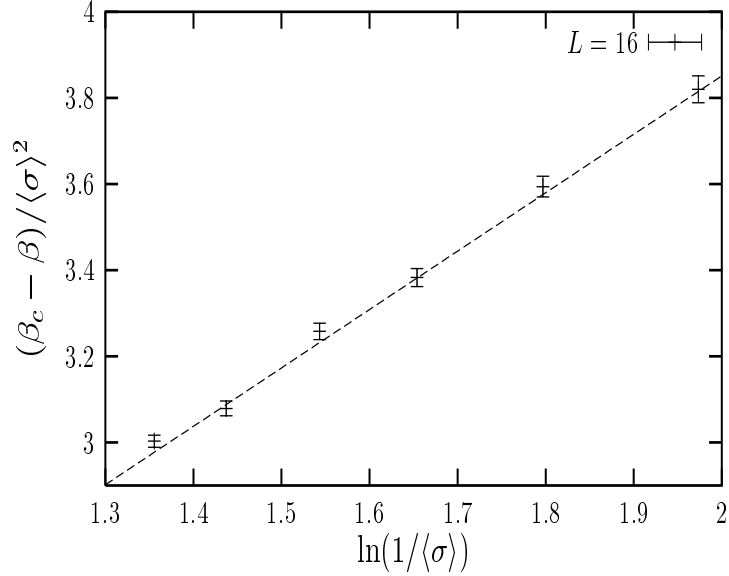
11

Figure 7: $(\beta_c - \beta)/\langle\sigma\rangle^2$ vs $\ln(1/\langle\sigma\rangle)$ at Four Fermi coupling $\lambda = 1.4$.

to FSS simulations below to remedy this limitation and obtain a better estimate for β_c.

5 24^4 **Simulations along the Vertical Line** $\lambda = 2.0$

Next consider simulations on larger lattices in the broken symmetry phase. In Fig. 8 we show the raw data from simulations on 24^4 lattices at a somewhat weaker four-fermi coupling $G = 0.5$. These larger lattices allowed us to run simulations closer to the critical point without suffering from large finite size effects. The algorithm was also somewhat better behaved at weaker four-fermi coupling $G = 0.5$. Of course we were not able to amass as high statistics in this case: one million sweeps per coupling were accumulated.

The raw data in Fig. 8 is fit with a simple power, $\langle\sigma\rangle = A(\beta_c - \beta)^{\beta_{mag}}$, and the parameters $A = 2.8(9)$, $\beta_c = 0.952(1)$, $\beta_{mag} = 0.77(10)$, were determined with $\chi^2/DOF = 1.18$. We again see that the best power law predicts a critical index β_{mag} higher than that of pure mean field theory, as in reference [3]. However,
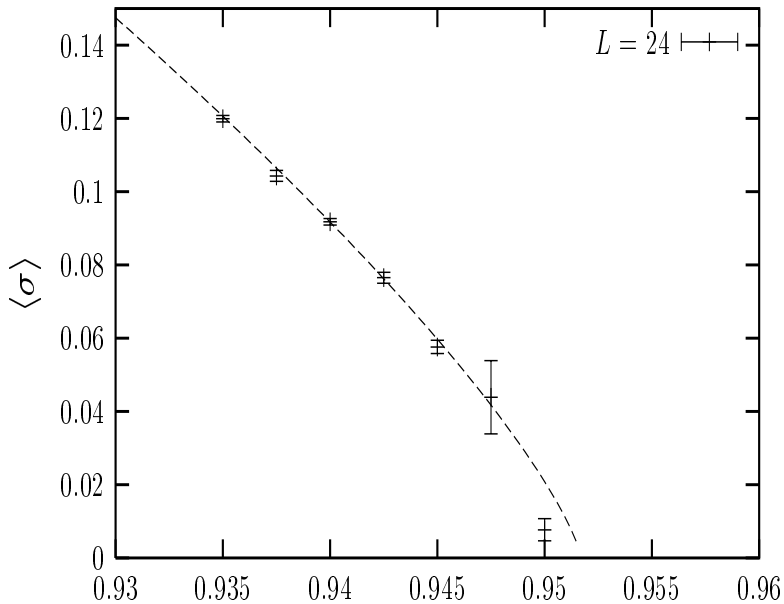
12

Figure 8: $\langle\sigma\rangle$ vs β at Four Fermi coupling $\lambda = 2.0$. The fit has the critical index $\beta_{mag} = 0.77(10)$.

the data is also well fit with the hypothesis of triviality. Fits to the form $\beta_c - \beta = A\langle\sigma\rangle^2(\ln(1/\langle\sigma\rangle) + B)$ gave the parameters $A = 0.21(10)$, $\beta_c = 0.951(1)$ and $B = -0.061(1)$ with a fine quality of fit $\chi^2/DOF = 0.78$. Following our presentation above, we plot $(\beta_c - \beta)/\langle\sigma\rangle^2$ against $\ln(1/\langle\sigma\rangle)$ in Fig. 9, which shows the importance of the logarithms and the deviation from pure mean field theory. As in Sec. 4 we find that the log-improved triviality fit is preferred to the power law form.

6 Results near the critical coupling

6.1 Background on Finite Size Scaling

In order to study the critical behavior of our theory arbitrarily close to the critical coupling we used FSS methods. FSS techniques first developed by Fisher [14] are important tools used in the determinations of critical exponents near second order phase transitions. The critical behavior of a system in the thermodynamic
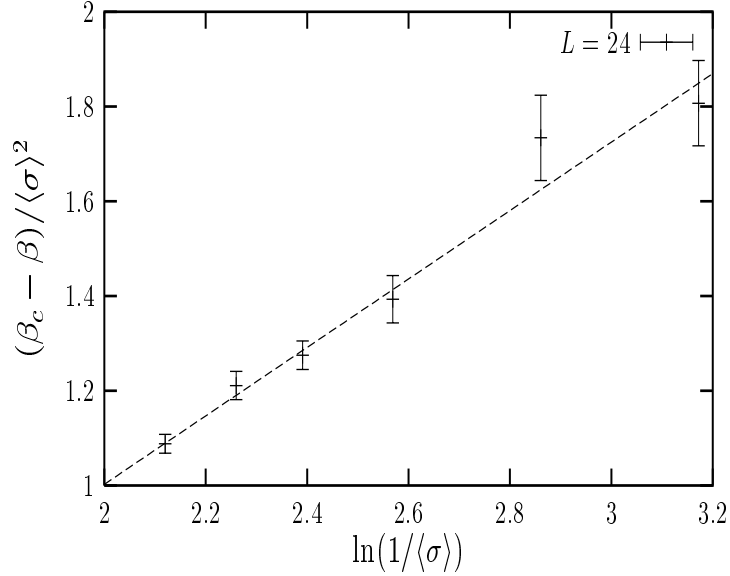
13

Figure 9: $(\beta_c - \beta)/\langle\sigma\rangle^2$ vs $\ln(1/\langle\sigma\rangle)$ at Four Fermi coupling $\lambda = 2.0$.

limit may be extracted from the properties of finite size systems by examining the size dependence of the singular part of the free energy density. According to FSS theory, for dimensionality d less than the upper critical dimension d_c, the singular part of the free energy is described phenomenologically by a universal scaling form,

$$F_s(t, m, L) = L^{-d}\mathcal{F}(tL^{1/\nu}, mL^{(\beta_{mag}+\gamma)/\nu}), \tag{8}$$

where m is the fermion bare mass and $t \equiv (\beta_c - \beta)$. The critical exponents ν, β_{mag} and γ are all the thermodynamic values for the infinite system. Scaling forms for various thermodynamic quantities can be obtained from appropriate derivatives of the free energy density. On a finite volume and with the fermion bare mass set to zero, the direction of symmetry breaking changes over the course of the run so the chiral condensate averages to zero over the ensemble. Another option is to introduce an effective order parameter $\Sigma \equiv \langle|\sigma|\rangle$, which in the thermodynamic limit is equal to the true order parameter $\langle\sigma\rangle$. The FSS scaling form for Σ determined

14

from Eq. 8 is

$$\Sigma = L^{-\beta_{mag}/\nu} f_\sigma(tL^{1/\nu}).\tag{9}$$

A standard method to measure β_c for a second order transition is to compute the Binder cumulant [15] for various system sizes. On sufficiently large lattices where subleading corrections from the finite lattice size L are negligible, the Binder cumulant $U_B(\beta, L)$, defined by

$$U_B \equiv 1 - \frac{1}{3}\frac{\langle|\sigma|^4\rangle}{\langle|\sigma|^2\rangle^2},\tag{10}$$

is given by $U_B = f_{BL}(tL^{1/\nu})$ and, therefore, at β_c it becomes independent of L.

Another quantity of interest is the susceptibility χ which, in the static limit of the fluctuation-dissipation theorem, is

$$\chi = \lim_{L\to\infty} V[\langle\sigma^2\rangle - \langle\sigma\rangle^2],\tag{11}$$

where V is the lattice volume. For finite systems this expression leads to the following finite-lattice estimates for χ:

$$\chi_1 = V\langle\sigma^2\rangle \quad \beta > \beta_c,\tag{12}$$

$$\chi_c = V[\langle\sigma^2\rangle - \langle|\sigma|\rangle^2] \quad \beta < \beta_c,\tag{13}$$

where the subscript c stands for "connected." Both relations should scale at criticality like $L^{\gamma/\nu}$. Furthermore, the maxima of χ_c in the scaling region should also obey $\chi_c^{\text{peak}} \sim L^{\gamma/\nu}$.

Furthermore, logarithmic derivatives of $\langle|\sigma|^n\rangle$ can give additional estimates for ν. It is easy to show that

$$D_n \equiv \frac{\partial}{\partial\beta}\ln\langle|\sigma|^n\rangle = \left[\frac{\langle|\sigma|^n P\rangle}{\langle|\sigma|^n\rangle} - \langle P\rangle\right],\tag{14}$$

where P is the plaquette, has a scaling relation

$$D_n = L^{1/\nu} f_{D_n}(tL^{1/\nu}).\tag{15}$$

15

Other related quantities useful in determining the critical exponent ν can be defined from logarithms of derivatives of $\langle \sigma^n \rangle$ [16]. In our analysis we will consider

$$Q \equiv 2[\sigma^2] - [\sigma^4], \tag{16}$$

where

$$[\sigma^n] \equiv \ln \frac{\partial \langle \sigma^n \rangle}{\partial \beta}. \tag{17}$$

One can easily show that

$$Q \simeq \frac{1}{\nu} \ln L + \mathcal{Q}(tL^{1/\nu}). \tag{18}$$

The above FSS relations rely on the traditional FSS hypothesis that in the vicinity of the critical coupling the behavior of the system is determined by the scaled variable L/ξ, where ξ is the correlation length. The standard FSS hypothesis fails for $d \geq d_c$. A modified hypothesis for $O(N)$-symmetric Φ^4 theories in four dimensions was proposed in [17], where it was shown that in the vicinity of the critical coupling the actual length of the finite size system is replaced by its correlation length $\xi_L(0) \propto L(\ln L)^{\frac{1}{4}}$, independent of N. However, as shown in [8] and demonstrated numerically in earlier sections of this paper, the logarithmic triviality in fermionic field theories such as the NJL model and QED is manifested in a different way from the triviality in purely bosonic theories. The logarithmic corrections in the scaling relations of QED are expected to be in the denominator of the scaling functions, whereas in Φ^4 theory they are in the numerator. The same is expected in the FSS relations of various thermodynamic quantities. By generalizing the Privman-Fisher ansatz for the scaling relation of the singular part of the free energy, the scaling function for $F_s(t, m_0, L)$ becomes

$$F_s(t, m_0, L) = L^{-d} \mathcal{F}(tL^2 \ln^p L, m_0 L^3 \ln^q L). \tag{19}$$

Consequently, the log-improved FSS relations for the effective order parameter and the susceptibility obtained from appropriate derivatives at zero fermion mass are,

$$\Sigma = L^{-1} \ln^q L f_\sigma(tL^2 \ln^p L), \tag{20}$$

$$\chi = L^2 \ln^{2q} L f_\chi (t L^2 \ln^p L). \tag{21}$$

In the next sections we will present our attempts to extract the critical exponents and to check consistency with log-improved scaling. We studied the FSS behavior of several observables in order to compare different results and reach conclusions.

6.2 Analysis of the Binder cumulant

In the vicinity of β_c we can expand the Binder cumulant and find

$$U_B(\beta, L) \simeq U_* + U_1(\beta_c - \beta)L^{1/\nu}. \tag{22}$$

By fitting this relation to data in the range $1.2875 \leq \beta \leq 1.375$ and lattice sizes $L = 8, .., 16$ we found $\nu = 0.49(10)$, $\beta_c = 1.356(7)$ and $U_* = 0.153(26)$ with $\chi^2/DOF = 1.6$. The measured value of the critical exponent ν is consistent with the mean field prediction $\nu = 1/2$, although the error is relatively large. More measurements of ν with better precision are presented below. The location of the critical point $\beta_c = 1.356(7)$ refines the estimates found from the broken symmetry fits given earlier. Since those studies were done far from β_c, a small discrepancy is not surprising.

6.3 Analysis of effective order parameter

In this section we discuss the FSS analysis for the effective order parameter Σ. We fit our data to $\Sigma_{\beta_c} = aL^{-\beta_{mag}/\nu}$ for three values of $\beta = 1.325, 1.350$ and 1.393, which are close to the value $\beta_c = 1.356$ extracted from the analysis of $U_B(L, \beta)$. The results are presented in Table 1 and plotted in Fig. 11. We conclude that β_c is close to 1.350 and the ratio $\beta_{mag}/\nu = 1.14(6)$ at this value of β is also close to the mean field result $\beta_{mag}/\nu = 1$.

We also fit all the data in the vicinity of the transition to a single scaling function obtained from the Taylor expansion of Eq. 9, up to a linear term,

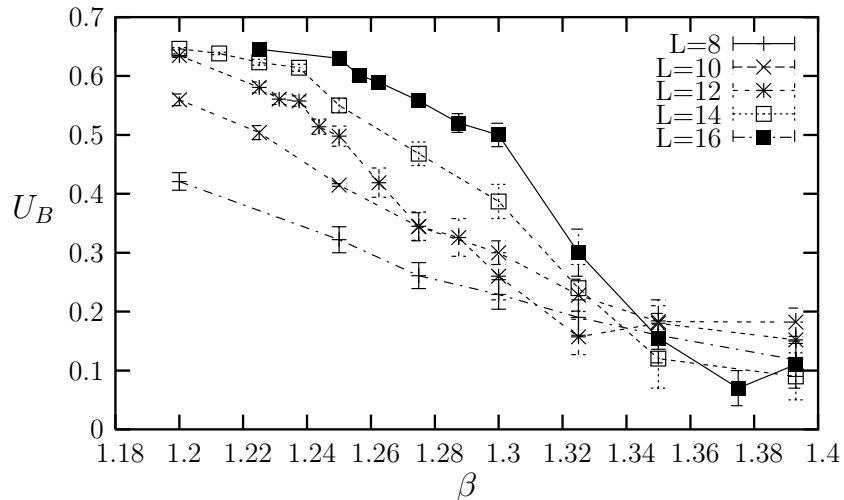$$\Sigma \simeq [c_1 + c_2(\beta_c - \beta)L^{1/\nu}]L^{\beta_{mag}/\nu}. \tag{23}$$

17

Figure 10: Binder cumulant versus coupling for different lattice sizes.

After fixing $\beta_c = 1.356$ we obtained the values of β_{mag}/ν and ν. When all the three values of the coupling ($\beta = 1.325, 1.350$ and 1.393) for $L = 8, ..., 16$, and an extra coupling $\beta = 1.375$ for $L = 16$, are included in the fit we get $\beta_{mag}/\nu = 1.13(4)$ and $\nu = 0.48(8)$ with $\chi^2/DOF = 1.4$. For the same data set and for fixed $\beta_c = 1.330$ (which is the value of the critical coupling obtained from the broken phase analysis) we get $\beta_{mag}/\nu = 0.95(5)$ and $\nu = 0.56(8)$ with $\chi^2/DOF = 1.3$.

In order to check whether our results are consistent with log-improved mean field scaling, we fit Σ to Eq. 20. The results are summarized in Table 2 and plotted in Fig. 12. The best fit is at $\beta = 1.350$ with $p = -0.34(14)$. The negative sign of p is consistent with the scenario of log-triviality in fermionic field theories [13].

6.4 Analysis of susceptibility

First, we fit χ_1 (Eq. 12) as a function of L at different values of $\beta = 1.325, 1.350$ and 1.393. The results are displayed in Fig. 13 and Table 3. It is clear from these
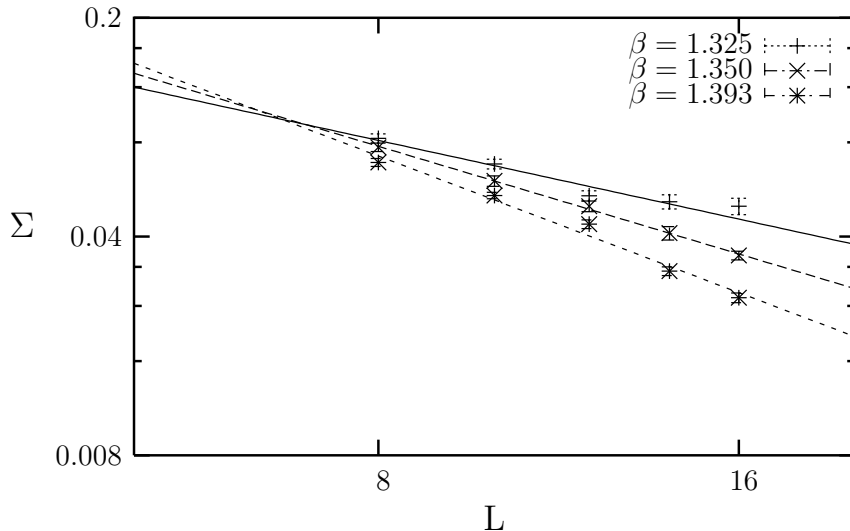
Figure 11: Σ vs. L for different values of β.

results that the critical coupling is close to $\beta = 1.350$ in agreement with analyses presented in previous paragraphs. The measured value of $\gamma/\nu = 1.76(14)$ is close to its mean field value of 2. We also fit χ_1 in the vicinity of the transition to the linear expansion of $\chi(L, \beta)$ around β_c.

$$\chi_1(L, \beta) \simeq [c_1 + c_2(\beta_c - \beta)L^{1/\nu}]L^{\gamma/\nu}. \tag{24}$$

After fixing the critical coupling to the value extracted from the broken phase analysis ($\beta_c = 1.330$) we get $\nu = 0.66(9)$ and $\gamma/\nu = 2.15(9)$ with $\chi/\text{DOF} = 1.3$, whereas after fixing β_c to the value extracted from the U_B analysis we get $\nu = 0.51(7)$ and $\gamma/\nu = 1.87(8)$ with the same χ^2/DOF as before. Furthemore, we fit the data to $\chi_1 \simeq aL^2(\ln^{2p}L)$ in order to check whether the data are consistent with log-improved mean field scaling. The results displayed in Table 5 provide good evidence that the log-improved scaling relation describes the data well and that $\beta_c \simeq 1.350$. The measured value $p = -0.28(16)$ is compatible with the result extracted from log-improved fits of Σ discussed in the previous section.
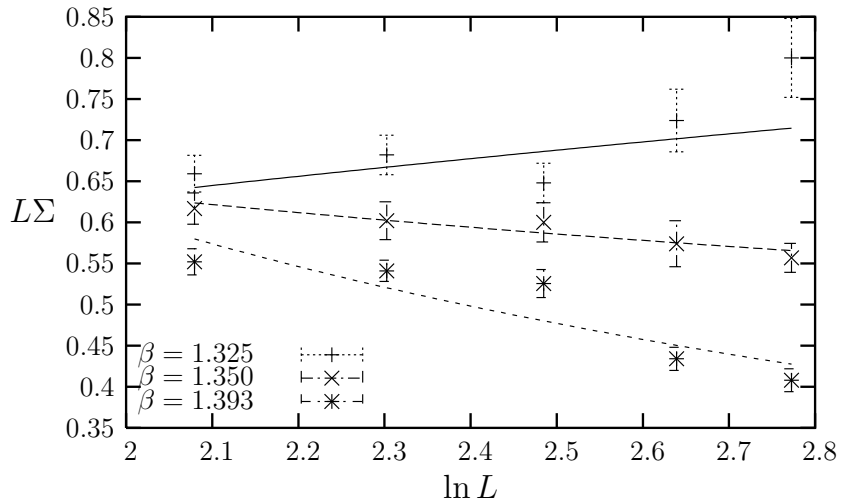
19

Figure 12: Fits to $L\Sigma = a \ln^p L$ for different values of β near the transition.

We repeated the above analysis for the connected susceptibility χ_c. The results presented in Table 5 indicate clearly that β_c is close to $\beta \simeq 1.350$ with the value $\gamma/\nu = 1.70(11)$ close to the mean field result. The results of fits to the log-improved FSS relation are summarized in Table 6. Again the results provide significant evidence that β_c is close to 1.350 and $p = -0.36(13)$ which is consistent with previous measurements of p. We also fitted the peaks of χ_c to $\chi_c^{\text{peak}} \sim L^{\gamma/\nu}$ and got $\gamma/\nu = 1.99(16)$ in good agreement with the mean field prediction. The data and the fitting function are shown in Fig. 14.

6.5 Analysis of D_j and Q

To make a further check of our results for the exponent ν, we studied the finite size scaling properties of logarithmic derivatives of $\langle|\sigma|^n\rangle$ defined in Eq. 14. We fit $D_j \sim L^{1/\nu}$ for $j = 1, 2$, and 3 at different values of the gauge coupling and for $L = 8, ..., 14$. We note that the data generated on 16^4 lattices were noisy and therefore could not be included in the fits. The results for the exponent ν and the
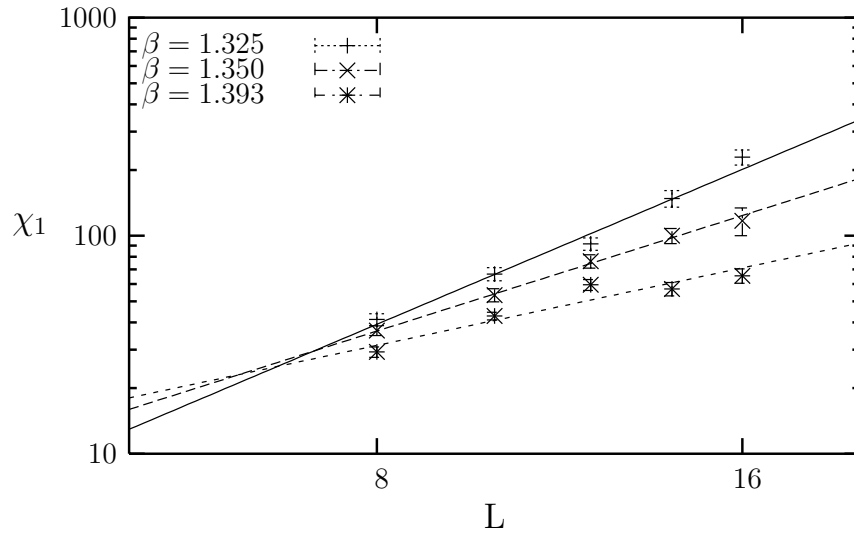
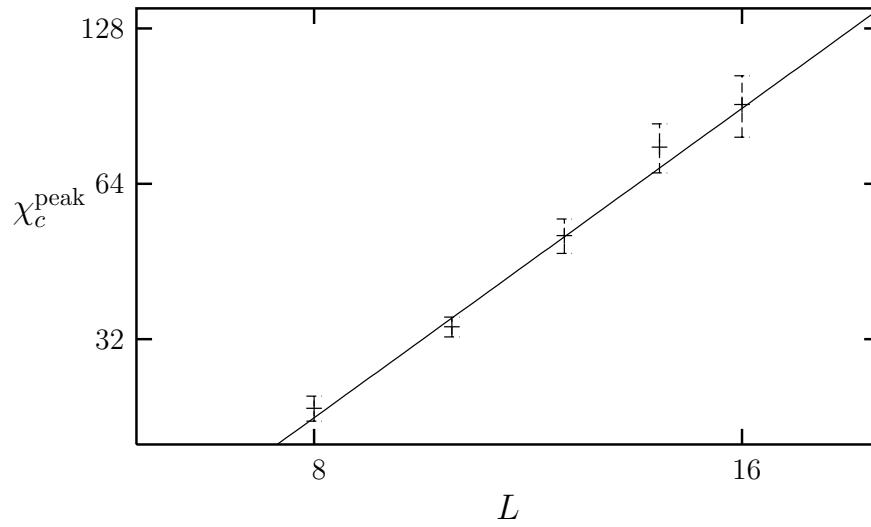Figure 13: Susceptibility χ_1 vs. L for different values of β.

Figure 14: Peaks of connected susceptibility χ_c vs. L.

21

quality of each fit are shown in Tables 7,8,9. ithe values of ν are in very good agreement with the mean field prediction $\nu = 0.5$. Although for these values of gauge coupling ν do not have a significant dependence on β, the qualities of the fits indicate that $\beta_c \simeq 1.350$ which is in agreement with results presented in previous paragraphs. Our attempts to fit the data to log-improved FSS mean field scaling laws $D_j \sim L^2 \ln^p L$ did not give any signal for p.
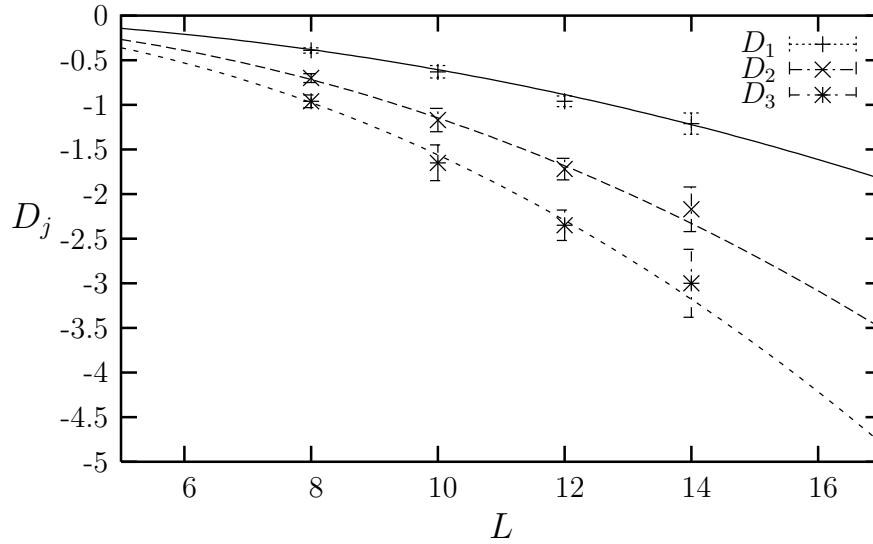

Figure 15: D_1, D_2 and D_3 vs. L at $\beta = 1.350$.

Furthermore, we fit all the data ($\beta = 1.325, 1.350, 1.393$) to the linear expansion of the FSS relation

$$D_j(\beta, L) \simeq c_{1j}L^{1/\nu} + c_{2j}(\beta_c - \beta)L^{2/\nu}, \tag{25}$$

with fixed $\beta_c = 1.356$. The results are summarized in Table 10 and are in good agreement with the mean field result although the quality of each fit is not as good as before.

Finally, a fit to the linear expansion of the observable Q (defined in Eq. 18)

$$Q \approx \frac{1}{\nu} \ln L + c_1 + c_2(\beta_c - \beta)L^{1/\nu} \tag{26}$$

22

for $\beta = 1.300, ..., 1.393$, $L = 8, ..., 14$ and fixed $\beta_c = 1.356$ gives $\nu = 0.52(3)$ and $\chi^2/DOF = 1.5$, in good agreement with all the measurements for ν presented in previous paragraphs.

7   Conclusions

We have presented evidence for the logarithmic triviality of the chiral transition line in compact QED with four species of fermions. A weak four-fermi interaction was employed in the action so that massless fermions could be simulated directly, thus avoiding the need to extrapolate raw data to the chiral limit. χQED allowed us to use the simplest single variable finite size scaling fits to the data. Since the four-fermi interaction is irrelevant in four dimensions and since the full model χQED is found to be logarithmically trivial, this study constitutes strong evidence that the continuum limit of the standard compact lattice QED model is also logarithmically trivial.

Finite size scaling proved to be an effective approach to deciding the physics issues inherent in these models. The FSS analyses provide strong evidence that the critical exponents are the mean field theory ones. Especially in the case of ν the analyses of various observables show in a consistent manner that ν is very close to 0.5. The broken phase data at different values of the four-fermi coupling also favor fermionic log-improved mean field scaling over the interacting field theory scenario.

Acknowledgments

Table 1: Results from fits to $\Sigma = aL^{-\beta_{mag}/\nu}$.

β	β_{mag}/ν	a	χ^2/DOF
1.325	0.84(8)	0.46(9)	2.1
1.350	1.14(6)	0.84(12)	0.16
1.393	1.45(5)	1.48(20)	4.6

Table 2: Results from fits to $\Sigma = aL^{-1}\ln^p L$.

β	a	p	χ^2/DOF
1.325	0.49(8)	0.37(19)	2.2
1.350	0.80(10)	-0.34(14)	0.20
1.393	1.26(14)	-1.06(13)	5.4

Table 3: Fits for $\chi_1 = aL^{\gamma/\nu}$.

β	a	γ/ν	χ^2/DOF
1.325	0.29(10)	2.36(14)	2.0
1.350	0.94(30)	1.76(14)	0.12
1.393	2.7(7)	1.18(11)	4.0

Table 4: Results from fits to $\chi_1 = aL^2(\ln^{2q} L)$.

β	a	p	χ^2/DOF
1.325	0.33(10)	0.41(17)	2.2
1.350	0.86(23)	-0.28(16)	0.13
1.393	2.06(45)	-0.97(13)	4.7

Table 5: Results from fits to $\chi_c = aL^{\gamma/\nu}$.

β	a	γ/ν	χ^2/DOF
1.325	0.056(15)	2.51(11)	31.3
1.350	0.36(9)	1.70(11)	0.9
1.393	0.80(18)	1.23(9)	4.5

Table 6: Results from fits to $\chi_c = aL^2(\ln^{2p} L)$.

β	a	p	χ^2/DOF
1.325	0.11(3)	0.30(17)	45.6
1.350	0.33(7)	-0.36(13)	0.9
1.393	0.62(12)	-0.91(11)	5.1

Table 7: Results of fits to $D_1 \sim L^{1/\nu}$

β	ν	χ^2/DOF
1.325	0.46(4)	1.1
1.350	0.48(4)	0.4
1.393	0.47(6)	3.3

Table 8: Results of fits to $D_2 \sim L^{1/\nu}$

β	ν	χ^2/DOF
1.325	0.47(4)	1.0
1.350	0.47(5)	0.3
1.393	0.48(7)	2.8

Table 9: Results of fits to $D_3 \sim L^{1/\nu}$

β	ν	χ^2/DOF
1.325	0.49(4)	1.0
1.350	0.47(5)	0.3
1.393	0.51(7)	2.3

Table 10: Results of fits to eq. 25.

	ν	χ^2/DOF
D_1	0.49(3)	2.5
D_2	0.51(3)	2.0
D_3	0.51(3)	1.9

References

[1] M. Baig, H. Fort, S. Kim, J. B. Kogut and D.K. Sinclair, Phys. Rev. **D48**, R2385 (1993); *ibid.* **D51**, 5216 (1995).

[2] S. Kim, J.B. Kogut and M.-P. Lombardo, Phys. Lett. **B502**, 345 (2001); Phys. Rev. **D65**, 054015 (2002).

[3] J. B. Kogut and C.G. Strouthos, Phys. Rev. **D67**, 034504 (2003).

[4] S. Hands and J. B. Kogut, Nucl. Phys. **B462**, 291 (1996).

[5] R. Myerson, T. Banks and J. B. Kogut, Nucl. Phys. **B129**, 493 (1977).

[6] K.G. Wilson, Phys. Rev. **D14**, 2455 (1974).

[7] Y. Cohen, S. Elitzur and E. Rabinovici, Nucl. Phys. **B220**, 102 (1983).

[8] S. Kim, A. Kocić and J.B. Kogut, Nucl. Phys. **B429**, 407 (1994).

[9] E. Dagotto and J.B. Kogut, Phys. Rev. Lett. **59**, 617 (1987).

[10] G. Arnold, B. Bunk, Th. Lippert and K. Schilling, hep-lat/0210010.

[11] C.N Leung, S.T. Love and W.A. Bardeen, Nucl. Phys.**B327**, 649(1986).

[12] S. Duane and J. B. Kogut, Phys. Rev. Lett. **55**, 2774 (1985).

[13] A. Kocić and J. Kogut, Nucl. Phys. B **422**, 593 (1994).

[14] M.E. Fisher, in *Critical Phenomena*, edited by M.S. Green (Academic, New York, 1971); M.E. Fisher and M.N. Barber, Phys. Rev. Lett. **28**, 1516 (1972); M.N. Barber, in *Phase Transitions and Critical Phenomena*, edited by C. Domb and J. Lebowitz (Academic, New York, 1983), Vol. 8; V. Privman (editor) *Finite Size Scaling and Numerical Simulations* (World Scientific, Singapore, 1990).

[15] K. Binder, Z. Phys. **B43**, 119 (1981).

[16] K. Chen, A.M. Ferrenberg and D.P. Landau, Phys. Rev. **B48**, 3249 (1993).

[17] R. Kenna and C.B. Lang, Phys. Lett. **B264**, 396 (1991); Nucl. Phys. **B393**, 461 (1993) 461; *ibid.* **411**, 340 (1994) (*Erratum*); Phys. Rev. **E49**, 5012 (1994); R. Kenna, arXiv:hep-lat/0405023.